Well-balanced energetic cocrystals of H_5IO_6/HIO_3 achieved by a small acid-base gap

Jichuan Zhang, Joseph P. Hooper, Jiaheng Zhang, Jean'ne M. Shreeve

PII: S1385-8947(20)32751-0
DOI: https://doi.org/10.1016/j.cej.2020.126623
Reference: CEJ 126623

To appear in: *Chemical Engineering Journal*

Received Date: 1 June 2020
Revised Date: 23 July 2020
Accepted Date: 8 August 2020

Please cite this article as: J. Zhang, J.P. Hooper, J. Zhang, J.M. Shreeve, Well-balanced energetic cocrystals of H_5IO_6/HIO_3 achieved by a small acid-base gap, *Chemical Engineering Journal* (2020), doi: https://doi.org/10.1016/j.cej.2020.126623

Well-balanced energetic cocrystals of H_5IO_6/HIO_3 achieved by a small acid-base gap

Jichuan Zhang,[1,2,3] Joseph P. Hooper,[4] Jiaheng Zhang,[2,3]* Jean'ne M. Shreeve[1]*

[1]Department of Chemistry, University of Idaho, Moscow, Idaho 83844-2343, USA.

[2]Research Centre of Flexible Printed Electronic Technology, Harbin Institute of Technology, Shenzhen, 518055, China.

[3]Zhuhai Institute of Advanced Technology Chinese Academy of Sciences, Biomaterials Research Center, Zhuhai, 519003, China.

[4]Department of Physics, Naval Postgraduate School, Monterey, California 93943, United States

Supporting Information

ABSTRACT: Achieving a balanced oxidant-to-fuel ratio remains a challenge in the field of energetic materials. Now, oxygen-rich acids, H_5IO_6/HIO_3 were combined with three weakly basic energetics (btrz: 4,4'-bis-1,2,4-triazole; atrz: 4,4'-azo-1,2,4-triazole; ICM-102: 2,4,6-triamino-5-nitropyrimidine-1,3-dioxide) to form four cocrystals (**1**: H_5IO_6/btrz; **2**: H_5IO_6/atrz; **3**: $2HIO_3$/atrz; and **4**: HIO_3/ICM-102) through the close acid-base gap of two precursors. The oxygen balances of the four cocrystals increased significantly, especially cocrystal **3**, where its available oxygen atoms provided by the two HIO_3 molecules is 5. Simple preparation, 49.2% iodine content, and excellent detonation performance of cocrystal **3** makes it a promising energetic biocidal agent. Cocrystal **4** shows potential as both a biocidal agent and energetic material. This work provides a new route for preparing cocrystals and broadens application of oxidants for the development of well-balanced energetic materials.

1 Introduction

Energetic materials (including explosives, propellants, pyrotechnics, and other functional agents, etc.), which release a large amount of chemical energy in a short time, play an irreplaceable role in modern society.[1] An ideal energetic compound should convert H and C into H_2O and CO_2, respectively, completely (oxygen balance: OB, which describes the excess or deficiency of oxidant to fuel) during the explosive reaction. However, the oxidant carried by a vast majority of energetic compounds is often very deficient,[2-4] which seriously limits the energy output.[5] Traditional methods to enhance the OB include the introduction of NO_2, N-O, and di/trinitromethyl groups at the N or C sites in an energetic skeleton through organic synthesis. These methods involve multi-step reactions and harsh conditions (such as concentrated acids and low or high temperatures), which not only increase the danger, but also produce large amounts of organic waste and waste acids (Scheme 1).[6-10]

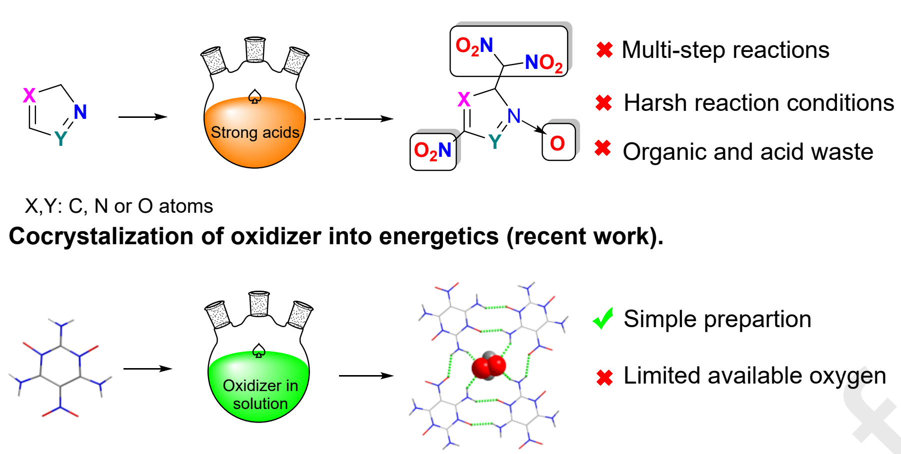

Scheme 1. Methods of enhancing oxygen balance in energetic materials.

In the past decades, cocrystal engineering has drawn extensive interest in energetic materials because it combines the respective advantages (high detonation properties, low sensitivities) of the two precursors.[11-14] The recent development of energetic cocrystals by embedding oxidants (e.g., H_2O_2, ammonium dinitramide (ADN), or N_2O) into energetics appears particularly promising in resolving the problem of negative OBs.[15-19] For example, the OB of cocrystal PDO-ADN (PDO: pyridine dioxide) increased to -18.0% from -114.3% for PDO through cocrystallization of ADN with PDO, which, along with a simple preparative method and excellent detonation performance makes PDO-ADN a promising energetic material.[17] However, large amounts of concentrated H_2SO_4 and HNO_3 and a low reaction temperature are required to prepare ADN.[20] Hydrogen peroxide and N_2O provide limited available oxygen (Scheme 1). Approaching zero for OBs is the goal of energetic materials. Therefore, significant improvement of the OB through a simple method is currently an attractive challenge in this field.

Research has shown that unlike in the case of salts, an important criterion for the formation of cocrystals is that the acid-base gap of the two precursors should not be too large. For example, in acid-base systems, if there is a strong acid ($HClO_4$, HNO_3, etc.) or a strong base (NaOH, KOH, etc.) involved, salts form.[21-22] As representative of weak acids, carboxylic-based compounds form salts with ammonia and guanidine, while they form cocrystals with weaker Lewis bases (such as amide-based compounds, N-heterocycles).[23-25] It is likely that as the acid-base gap of the two precursors becomes smaller, it is more difficult for the base (acid) to protonate (deprotonate),[26] leading to the formation of a cocrystal. From this point, the acids and bases, whose acid-base gap is small, are the two classes of potential starting materials used for forming cocrystals. Considering that an oxygen acid would be able to provide more oxygen for energetic materials, H_5IO_6 and HIO_3 were readily available first choices. Additionally, the product, I_2, released from iodine compounds after initiation, is a biocidal agent, which can kill harmful microorganisms which may be present in the environment.[27] This method of introducing iodine via cocrystallization is simpler than traditional organic syntheses.[28-31]The pKas of H_5IO_6 and HIO_3 are 1.64 and 0.8,[32] respectively. HIO_3 approaches being a strong acid (strong acid: pKa < 0).[33] It is expected that the weaker bases can potentially form cocrystals with H_5IO_6 and HIO_3. Btrz (4,4'-bis-1,2,4-triazole), atrz (4,4'-azo-1,2,4-triazole), and ICM-102 (2,4,6-triamino-5-nitropyrimidine-1,3-dioxide), are seen as very weak bases for the following reasons: 1) atrz forms cocrystals with the weak acid LLM-116 (4-amino-3,5-dinitropyrazole, pKa: 3.42), which forms salts with a series of triazole-based weak bases, the analogue (btrz) of atrz forms nitrate and perchlorate salts;[34-37] 2) ICM-102 forms a cocrystal with H_2O_2 (a type of weak acid), it forms salts with $HClO_4$ and HNO_3.[19] In this study, four cocrystals were formed: **1**, H_5IO_6/btrz; **2**, H_5IO_6/atrz; **3**, $2HIO_3$/atrz; and **4**, HIO_3/ICM-102 were synthesized (Scheme 2). The rationale for the formation of cocrystals was examined by NBO (Natural Bond Orbital) charge distribution, and their crystal structures as well as physiochemical properties were investigated extensively.

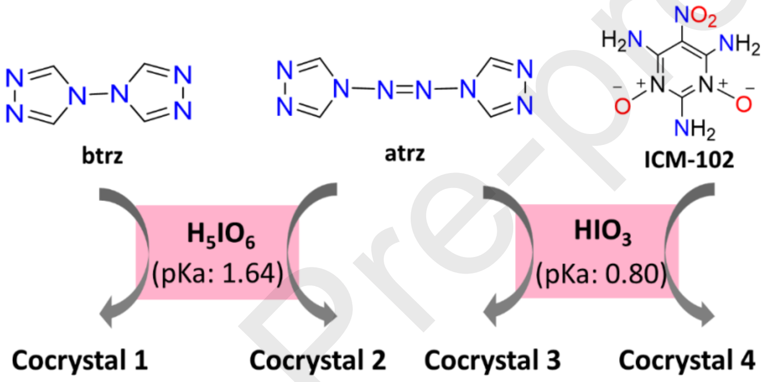

Scheme 2. Synthesis of cocrystals **1-4**.

2 Experimental section

Safety Precautions.

Although none of the energetic compounds described herein has exploded or detonated accidentally in the course of this research, these materials should be handled with extreme care using the best safety practices.

General.

All reagents were purchased from AKSci or Alfa Aesar in analytical grade and were used as supplied. ^{1}H NMR and ^{13}C NMR spectra were recorded on a 300 MHz (Bruker AVANCE 300) nuclear magnetic resonance spectrometer. Chemical shifts for ^{1}H NMR and ^{13}C NMR spectra are given with respect to external $(CH_3)_4Si$ (^{1}H and ^{13}C). [D6] DMSO was used as a locking solvent unless otherwise stated. IR spectra were recorded using KBr pellets with a FT-IR spectrometer (Thermo Nicolet AVATAR 370). Density was determined at room temperature by employing a Micromeritics AccuPyc II 1340 gas pycnometer. Decomposition temperatures (onset) were recorded using a dry nitrogen gas purge and a heating rate of 5 °C min^{-1} on a differential scanning calorimeter (DSC, TA Instruments

Q2000). Elemental analyses (C, H, N) were performed with a Vario Micro cube Elementar Analyzer. Impact and friction sensitivity measurements were made using a standard BAM Fallhammer and a BAM friction tester.

Computational Methods.

Theoretical calculations of btrz, atrz and ICM-102 were performed by using the Gaussian 03 (Revision D.01) suite of scripts.[38] The geometric optimization, frequency analyses and NBO calculations of conventional CHNO-based compounds were completed by using the B3LYP functional with the 6-31+G** basis set. The NBO calculations of HIO_3 and H_5IO_6 were accomplished by using G2ECP(ZPE=MP2) method. Single energy points were calculated at the MP2/6-311++G** level of theory. For all of the compounds, the optimized structures were characterized to be true local energy minima on the potential-energy surface without imaginary frequencies. Isodesmic reactions were used to obtain the gas-phase heats of formation of btrz, atrz, and ICM-102 (Scheme S1). The gas-phase enthalpies of the building-block molecules were obtained by using the atomization method with the G2 ab initio calculations. For cocrystals, the solid-state heat of formation (HOF, $\Delta_f H°$) was calculated based on a Born–Haber energy cycle[39] with the following simplified equation for calculation:

$$\Delta_f H° \text{ (cocrystal, 298K)} = \Delta_f H° \text{ (precursor 1, 298K)} + n\Delta_f H° \text{ (precursor 2, 298K)} - \Delta H_{sub} \text{ (n = 1 or 2)}$$

The heat of sublimation can be estimated using the DFT method with the GGARPBE (revised Perdew Burke-Ernzerhof) exchange-correlation functional in Dmol3 program.[40-41]

Crystal Structure Analysis.

Cocrystals **1-4** (**1**, colorless chunk-shaped crystal with dimensions 0.15×0.10×0.09 mm^3; **2**, colorless chip-shaped crystal with dimensions 0.10×0.06×0.03 mm^3; **3,** colorless chunk-shaped crystal with dimensions 0.12×0.04×0.03 mm^3, and **4**, orange chunk-shaped crystal with dimensions 0.20×0.11×0.06 mm^3) were mounted on nylon loops with paratone oil, respectively. Data for these four crystals were collected using a Bruker APEX-II CCD diffractometer equipped with an Oxford Cryosystems low-temperature device, operating at T = 173(2) K.

Preparation of cocrystals 1-4.

General methods for preparing cocrystals **1**, **2**, and **4**, energetics (btrz/atrz/ICM-102) (1 mmol) was added to water (15 mL) at 60-70°C. Then H_5IO_6 or HIO_3 (0.228/0.176g; 1 mmol) was added with stirring at 60-70°C for 30 minutes. The solution was filtered, and two or three days later, a cocrystal precipitated at the bottom of the vial containing the filtrate.

The crystals were obtained by filtration, washed by a small amount of water (5 mL) and dried. The preparation of cocrystal **3** is the same as for **1**, with a molar ratio of HIO_3 to atrz of 2:1.

Cocrystal 1: Colorless crystal, yield: 63%. ^1H NMR (d6-DMSO): δ 9.16 (s, 5H), 6.42 (s, 4H) ppm. ^{13}C NMR (d6-DMSO): δ 142.65 ppm. IR (KBr): ν 3123, 2894, 2440, 1616, 1505, 1300, 1265, 1191, 1076, 1018, 965, 776, 646, 609 cm^{-1}. $C_4H_9IN_6O_6$ (364.07): Calcd: C 13.20, H 2.49, N 23.08 %. Found: C 13.29, H 2.60, N 22.89 %.

Cocrystal 2: Colorless crystal, yield: 65%. ^1H NMR (d6-DMSO): δ 9.43 (s, 5H), 6.08 (s, 4H) ppm. ^{13}C NMR (d6-DMSO): δ 138.39 ppm. IR (KBr): ν 3425, 3119, 2944, 2376, 1644, 1489, 1369, 1315, 1179, 1040, 934, 854, 765, 695, 619, 578 cm^{-1}. $C_4H_9IN_8O_6$ (392.09): Calcd: C 12.25, H 2.31, N 28.58 %. Found: C 12.23, H 2.36, N 28.95 %.

Cocrystal 3: Colorless crystal, yield: 76%. ^1H NMR (d6-DMSO): δ 9.44 (s, 2H), 5.79 (s, 4H) ppm. ^{13}C NMR (d6-DMSO): δ 138.41 ppm. IR (KBr): ν 3440, 3116, 2940, 2655, 2344, 1733, 1488, 1367, 1315, 1176, 1035, 926, 884, 854, 694, 617, 543 cm^{-1}. $C_4H_6I_2N_8O_6$ (515.97): Calcd: C 9.31, H 1.17, N 21.72 %. Found: C 9.37, H 1.21, N 22.20 %.

Cocrystal 4: Orange crystal, yield: 78%. ^1H NMR (d6-DMSO): δ 9.13 (s, 4H), 8.46 (s, 2H) ppm. ^{13}C NMR (d6-DMSO): δ 149.55, 146.86, 106.22 ppm. IR (KBr): ν 3354, 3176, 1643, 1500, 1404, 1303, 1203, 1073, 882, 764, 703, 645 cm^{-1}. $C_4H_7IN_6O_7$ (377.94): Calcd: C 12.71, H 1.87, N 22.23 %. Found: C 12.52, H 1.93, N 22.89 %.

3 Results and discussion

3.1 Single crystal structure.

Cocrystal **1** crystallized from water in the monoclinic space group (C 2/c), with four H_5IO_6 molecules and four btrz ligands in each unit cell (Figure 1a). One btrz molecule is trapped by seven H_5IO_6 molecules, and one H_5IO_6 is trapped by five btrz molecules (Figure S1). The calculated single crystal density of **1** is 2.278 g cm^{-3} at 173 K (Table S1). Two types of hydrogen bonds (H-bonds), N-H···O (1.873 and 2.027 Å) and O-H···N (2.358 and 2.384 Å), were formed. Because of the disordered H (50% occupancy) between the neighboring H_5IO_6 molecules, a special H···H bond has a length of 1.159 Å (Figure 1b). Structure **1** was bonded through a large number of H-bonds forming a 3D network (Figure S2).

Cocrystal **2** crystallized from water in the triclinic (P-1) space group with one H_5IO_6 and one atrz molecule in each unit cell (Figure 1c). Its calculated single crystal density is 2.354 g cm^{-3} at 173 K. Each H_5IO_6 molecule is trapped by four atrz molecules and two H_5IO_6 molecules through H-bonds, and each atrz molecule is trapped by four H_5IO_6 molecules through H-bonds (Figure 2d and Figure S3). Two types of H-bonds, N-H···O (2.311 and 2.340 Å) and O-H···N (1.991 and 2.041 Å), were formed. Similiarly for H_5IO_6 in cocrystal **1**, the H atoms between the neighboring H_5IO_6 molecules were also disordered, and two parallel H-bonds (1.947 Å) were formed between two neighboring

H_5IO_6 in **2** instead of special H···H bonds (Figure 1d). The structure was connected through numerous H-bonds that form a layered 3D network (layer-layer distance: 3.20 Å), in which H_5IO_6 serves as connecting nodes.

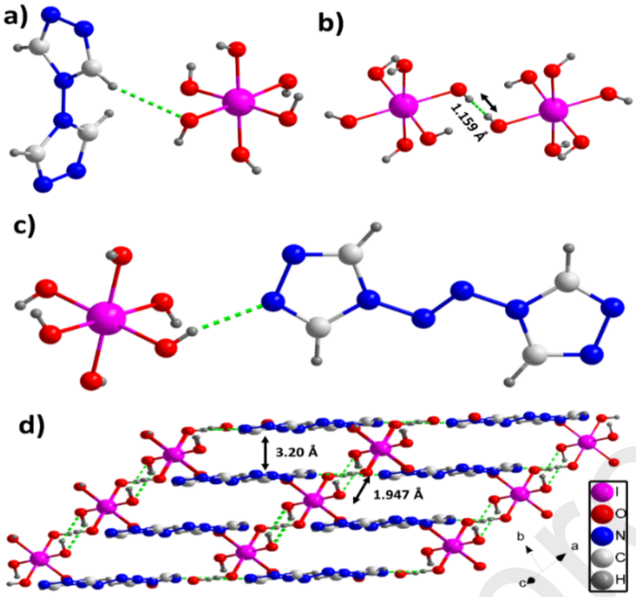

Figure 1. a and b) Single crystal structure and special H···H bond of **1**; c and d) Single crystal structure and packing mode of **2**

Cocrystal **3** also crystallized from water in the monoclinic (P21/c) space group; however, it is different from cocrystals **1** and **2** in that one atrz molecule combines with two HIO_3 molecules in each unit cell. The single crystal density of **3** is as high as 2.875 g cm^{-3} at 173 K, and only two symmetrical H-bonds (1.813 Å) formed between HIO_3 and atrz (Figure 2a). Cocrystal **3** shows a layer packing mode (layer-layer distance: 3.22Å) due to the coplanar atrz (Figure 2b).

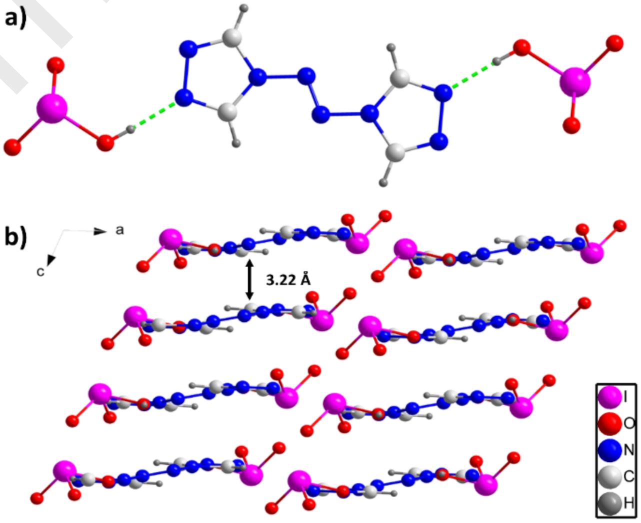

Figure 2. a) Single crystal structure of **3**; b) packing mode of **3**.

Cocrystal **4** crystallized from water in the triclinic (P-1) space group, with two ICM-102 molecules, two crystal waters, and two HIO_3 molecules in each unit cell. The calculated single crystal density of **4** is 2.521 g cm^{-3} at 173 K. It is interesting that coplanar ICM-102 has six intramolecular H-bonds with bond lengths of 2.019, 2.023, 2.210, 2.212, 2.260, and 2.320 Å, respectively (Figure 3a). Additionally, eight types of intermolecular H-bonds were formed among ICM-102, H_2O, and HIO_3 with bond lengths of 1.592, 1.933, 1.993, 2.035, 2.068, 2.165, 2.350, and 2.411 Å (Figure S4). Especially the H-bond length of 1.592 Å, which is among the shortest hydrogen bonds of energetic compounds.[6] Finally, the structure was connected through the special short H-bonds, forming a double-layered (H-bond connecting layer: 3.06Å and I-I layer:3.15Å, Figure 3b) 2D network.

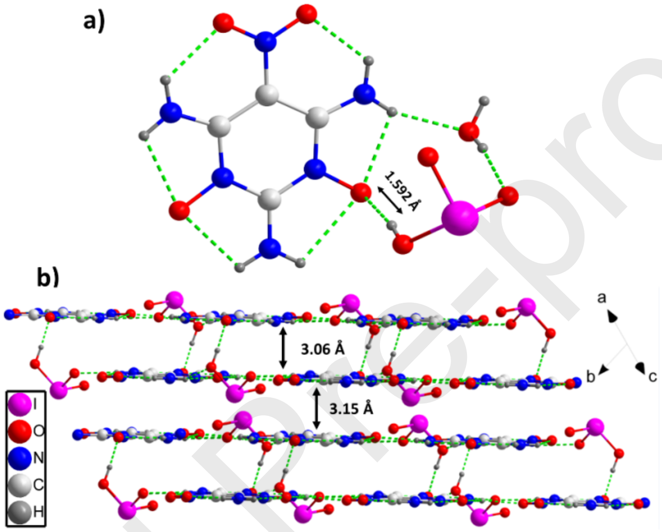

Figure 3. Single crystal structure, **4;** packing mode, **4**.

Usually, the acid-base property of a compound depends greatly on the NBO value; that is, the higher the NBO value of the proton, the more acidic the compound. On the contrary, the lower the NBO value of N or O that greater tendency to bind to protons, the stronger is the base.[42] For example, with a decrease in acidity in the order $HClO_4$ > HNO_3 > TNP (3,4,5-trinitro-1H-pyrazole) > DNP (3,5-dinitro-1H-pyrazole) > LLM-116 with pKa values of -10.0, -2.0, 2.35, 3.14, and 3.42 respectively,[9,35,37] the charge on their protons decreased with NBO values of 0.531, 0.522, 0.489, 0.482, and 0.480, respectively (Figure 4 and Figure S5-S13). Similarly, a change in the NBO value of the N atoms that readily bind to protons in guanidine, 3,5-diamino-1,2,4-triazole (DAT), 3-amino-1,2,4-triazole (3-AT), and 1,2,4-triazole (Tr) changes the basicity.[43-44] $HClO_4$, and HNO_3 form salts with any base as strong acids. DNPP (3,6-dinitropyrazolo[4,3-c] pyrazole) with an NBO value of the readily lost proton at 0.478 and whose acidity is supposed to be weaker than LLM-116 along with LLM-116 form salts with guanidine and DAT. DNPP and LLM-116 form cocrystals with 3-AT and atrz, respectively.[35,45,46] Hence, the investigation of NBO of the precursor can help understand the formation of cocrystals, as well as the acid-base properties of a compound.

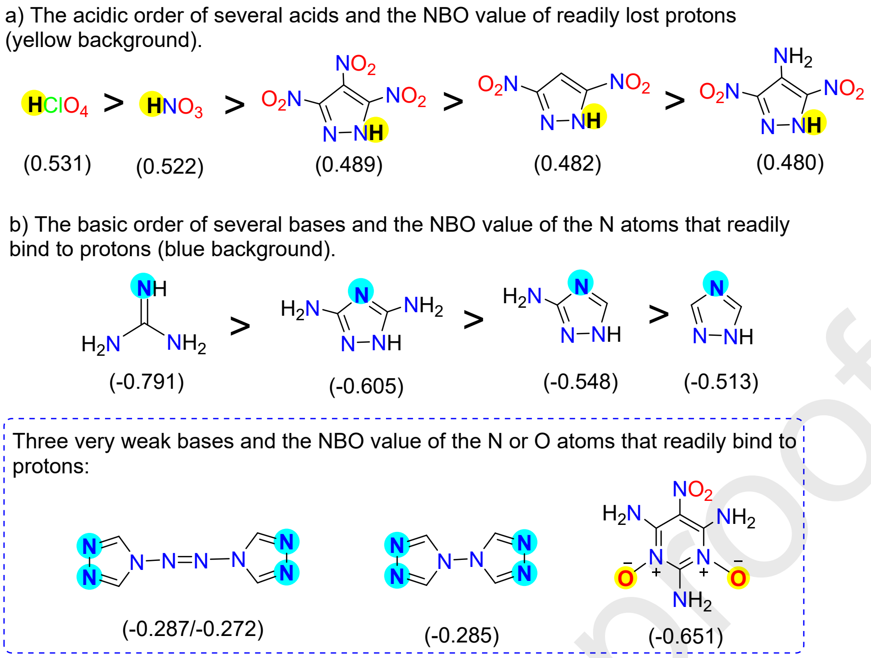

Figure 4. The order of acids and bases with their calculated NBO charges on protons and N/O atoms.

The NBO values of protons in H_5IO_6 and HIO_3 are 0.503 (average value) and 0.549, respectively (Figure S14). Their pKas are 1.64 and 0.80, respectively. Although the NBO value of the proton in HIO_3 is higher than those in $HClO_4$ and HNO_3, the acidity of HIO_3 is lower than $HClO_4$ and HNO_3. This arises from a delocalization effect of the larger I atom compared to CHNO atoms. Apparently, H_5IO_6 and HIO_3 are stronger acids than TNP, DNPP and LLM-116. HIO_3 is close to a strong acid (pKa < 0). Hence, the NBO values of N or O atoms that readily bind to protons in these three weak bases should be higher than those in DAT, 3-AT, and Tr. The calculated NBO values of corresponding N atoms in btrz and atrz are -0.285, -0.287/-0.272, respectively, which are obviously higher than those in DAT, 3-AT, and Tr. The NBO values of the corresponding two O atoms in ICM-102 are both -0.651, lower than that in H_2O_2 (-0.497), and much higher than that in H_2O (-0.995) (S15-18), which supports that btrz, atrz and ICM-102 are weak bases. It is interesting to note that the shortest H-bonds in cocrystal **3** (1.813 Å) and **4** (1.592Å) were apparently shorter than those in **1** (1.873Å) and **2** (1.947Å), this is possibly due to the fact that it is difficult for stronger HIO_3 to deprotonate in the cocrystal systems of **3** and **4**, leading to the formation of strong H-bonds. Therefore, more and more cocrystals with strong H-bonds are expected to be prepared based on the results in this work.

3.2 Physicochemical properties.

Anhydrous **1–4** (see Experimental section) were heated at 5 °C/ min^{-1} in a nitrogen atmosphere, and their decomposition temperatures (onset) were found to be 163 °C, 136 °C, 192 °C, and 181°C, respectively (Figures S19-

S22). It is interesting to observe that although atrz is more thermally stable than btrz,[47,48] the decomposition temperature of **1** is not only higher than that of **2**, but also higher than those of periodate-based organic compounds.[30] This may be because of the especially strong H···H interaction (short bond length of 1.159 Å), the short H-bond (1.873 Å) in **1,** and the two parallel H-bonds in **2** (1.947 Å) produced by the disordered H bonds which are longer than those in **1**. Hirshfeld surface analysis also shows that the distance of "soft" H···H interactions in **1** is as high as 0.4d (Figure 5), which is not only stronger than that in **2**, but also the strongest "soft" interaction ever reported.[6,7] Although in cocrystal **3**, one atrz molecule combines with two HIO_3 molecules, its decomposition temperature (192 °C) is higher than those of iodate-based organic compounds,[30] which is possibly because of the short H-bond (1.813 Å) and π-π interaction (layer distance ≈ 3.22 Å) between the two layers. Furthermore, the decomposition temperature of **4** is comparable to that of 2,4,6-triamino-5-nitropyrimidine-1,3-dioxide nitrate (177 °C),[19] which may arise because of the combination of multiple H-bonds, very short H-bond (1.592 Å), and strong π-π interaction (layer distance ≈ 3.06 and 3.15 Å). Generally, nitrates are more stable thermally than iodates. The impact sensitivities of **1–4** were determined as 28, 23, 8, and 35 J, respectively. Compound **1** is insensitive (>360 N) to friction stimulation, and the friction sensitivities of **2–4** are 120, 96, and 240 N, respectively. All the four cocrystals are less sensitive than the previously reported iodate and periodate-based compounds.[30] This may arise because of the especially strong H···H interactions, multiple (strong) H-bonds, and π-π interactions.

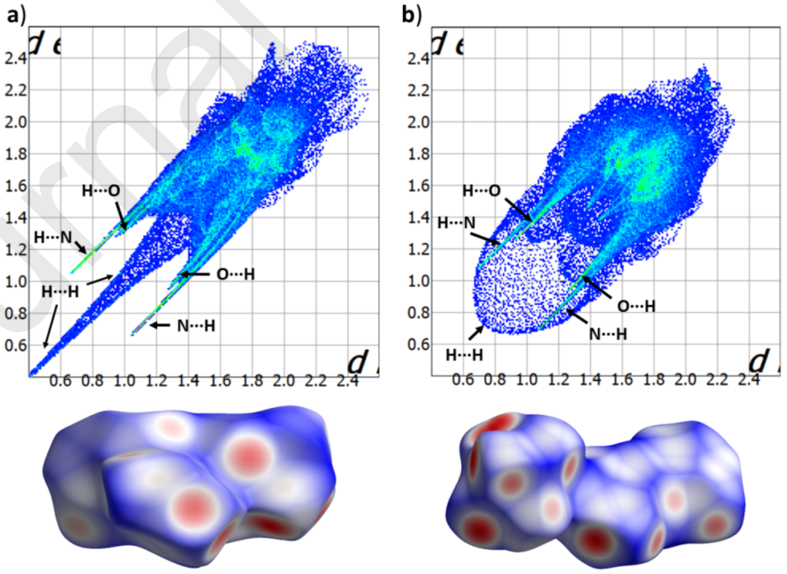

Figure 5. Two-dimensional fingerprint plots and Hirshfeld surfaces of (a) **1** and (b) **2**.

The packing densities of anhydrous **1–4**, measured using a pycnometer at room temperature, were 2.25, 2.31, 2.82, and 2.48 g cm^{-3}, respectively (Table 1). In particular, the densities of **3** and **4** are obviously higher than those with the same iodine content level.[28,31,49] This is, because the packing index of **3** and **4** are 77.7% and 79.5%, respectively, which are higher than the majority of organic compounds and of all reported energetic iodine compounds (see Supporting Information, Figure S23-S24). Because H_5IO_6 and HIO_3 are sources of more oxygen than N_2O and H_2O_2, the OBs of **1–4** were increased significantly to -28.5, -26.5, -15.5, and -14.8% from -117.5 (btrz), -97.6 (atrz), and -55.2% (ICM-102), respectively. The available oxygen atoms in **3** is 5 for each cocrystal molecule which is much higher than that provided by ADN-PDO (Figure 6).[17]

Table 1. Physicochemical properties of different energetic compounds.

Comp.	ρ ^{a} (g cm^{-3})	**OB** ^{b} (%)	**T$_{d}$** ^{c} (°C)	**IS**^{d} (J)	**FS** ^{e} (N)	**I** ^{f} (%)	$\Delta_f H^{o\,g}$ (kJ mol^{-1})	**D$_v$** ^{h} (m s^{-1})	**P** ^{i} (Gpa)
1	2.25	-28.5	163	28	>360	34.89	-575.5	6664	20.58
2	2.31	-26.5	136	23	120	32.40	-44.8	7538	29.52
3	2.82	-15.5	192	8	96	49.23	168.5	6960	30.68
4	2.48	-14.8	181	35	240	33.60	-437.4	7591	32.57
DIDNPT ^{j}	2.56	-41.4	323	7.4	>40	50.46	1192.7	5834	21.48
TNT ^{j}	1.65	-74.00	295	15	353	--	−31.7	6881	19.50

^{a} Experimental density at room temperature. ^{b} Oxygen balance (OB), calculated according to [OB = (O-2C-1/2H)1600/M]. ^{c} Decomposition temperature (onset). ^{d} Impact sensitivity (J). ^{e} Friction sensitivity (N). ^{f} Iodine content (%). ^{g} Enthalpy of formation (kJ mol^{-1}). ^{h} Detonation velocity (m s^{-1}). ^{i} Detonation pressure (Gpa). ^{j} Ref 28.

The iodine contents of **1-4** are 34.89, 32.40, 49.23 and 33.60%, respectively. The released I contents calculated by Cheetah (8.0 version) are 31.40, 29.07, 46.46, and 30.45, respectively, which were confirmed by experimental determinations (see Supporting Information). Compound **3**, with an iodine content is almost 50%, is a very promising biocidal agent. The enthalpies of formation of **1-4** were calculated to be -575.5, -44.8, 168.5 and -437.4 kJ mol^{-1}, respectively (Supporting Information). The detonation velocities of **1–4** were determined to be 6664, 7538, 6960 and 7591 m s^{-1}, respectively, and their detonation pressures are 20.58, 29.52, 30.68 and 32.57 Gpa, respectively. It is should be noted that the detonation properties of **2-4** are higher than those of TNT. The detonation velocity of **3** is higher than that of DIDNPT (2,6-diiodo-3,5-dinitro-4,9-dihydrodipyrazolo [1,5-a:5′,1′-d][1,3,5]triazine), the representative of compounds whose iodine content is about 50% [28,50,51] by almost 1100 m s^{-1} (Figure 6 and Table 1). This is the first compound where the detonation velocity is higher than that of TNT with an iodine content of about 50%. According to the empirical Kamlet formula, [52] detonation properties are dependent on density and heat of detonation. In detail, the detonation velocity (Vd) is proportional to the density and the quadruplicate of the heat of detonation, while the detonation pressure (P) is roughly proportional to the square of the density and square of the heat of detonation. Heat of detonation is dependent on heat of formation and oxygen balance. For I-based energetic materials, due to the large relative atomic mass of I, it is inverse to its detonation performance. These above reasons show that due to the higher heat of formation of **2** compared to **1**, the detonation properties of **2** are higher than those of 1. This is the case even though the density and oxygen balance for the two compounds are nearly the same. Compared to cocrystal **2**, **4** has a higher density and oxygen balance. Its detonation velocity is only slightly higher than that of **2**, likely caused by the low heat of formation of **4**. Cocrystal **3** has the highest density, as well as an excellent oxygen balance and a high heat of formation of these four cocrystals. Its detonation performance is lower than that of **4**, resulting from the fact that it has the highest I content among these four cocrystals. The excellent detonation properties of **1-4** are conducive to the diffusion of explosion products (I_2) over a larger range to effectively destroy more harmful microorganisms. In particular, the thermal stability and high iodine content (49.23%) makes **3** a promising energetic biocidal agent. Cocrystal **4** shows potential as both a biocidal agent and an HEDM.

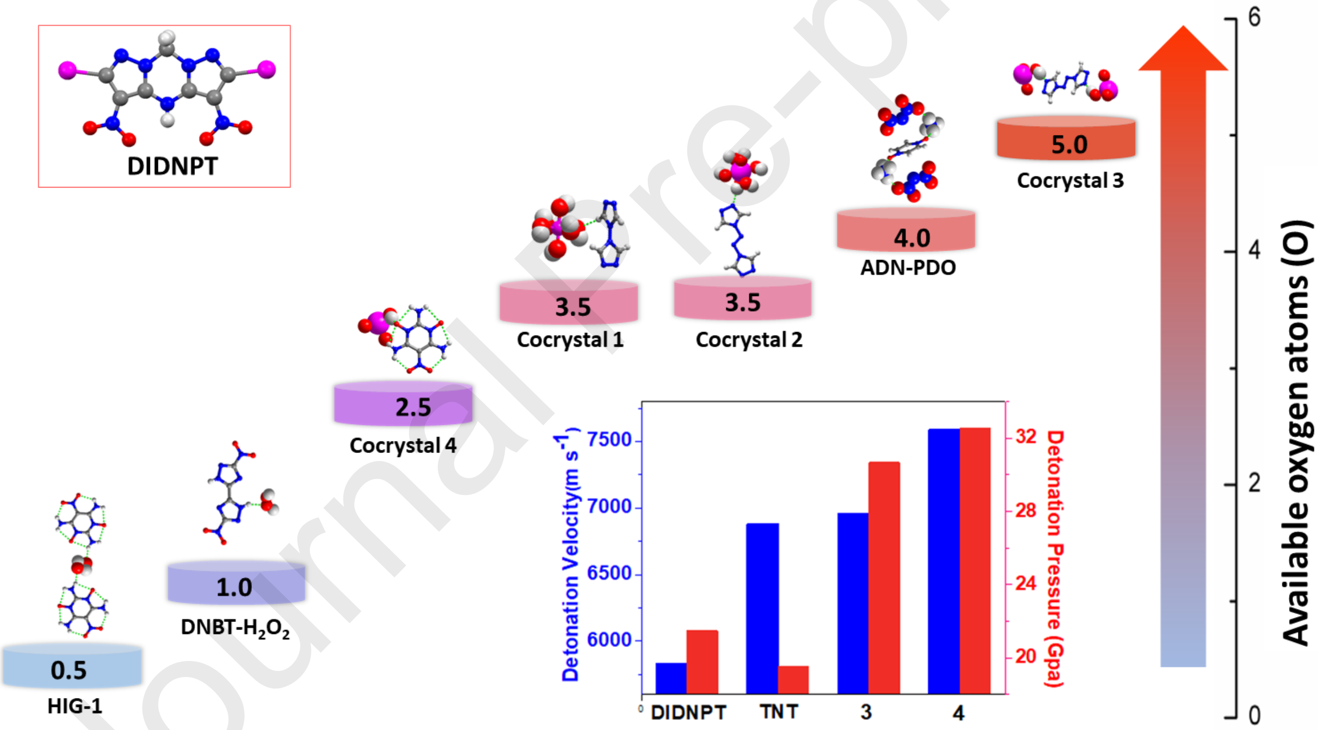

Figure 6. The available oxygen atoms provided by oxidants through cocrystallization (HIG-1: 2ICM-102·H_2O_2, DNBT: 3,3'-dinitro-5,5'-bis-1H- 1,2,4-triazole).

4 Conclusion

In this work, moderately strong acids, H_5IO_6 and HIO_3, were used as oxidants and combined with weakly basic energetics via cocrystallization of the small acid-base gap. The resulting four cocrystals **1–4** were characterized using single crystal X-ray diffraction analysis. Due to the oxygen-rich H_5IO_6 and HIO_3, the OBs of **1–4** were significantly large. Particularly, cocrystal **3** has the highest available number of oxygen atoms (5) provided by the oxidant through cocrystallization for each cocrystal molecule. A high iodine content (49.2%), ease of preparation, acceptable thermal stability, and excellent detonation properties make it a promising energetic biocidal agent. Cocrystal **4** shows potential not only as a biocidal agent, but also a high energy density material. This study expands the scope of oxidants for the development of well-balanced energetic materials comprised of many additional cocrystals with excellent properties resulting from the methodology developed here.

Supporting Information

Supplementary Information (Experimental method, additional figures and tables) is available in the online version of the paper(https://doi.org).

Corresponding Author

jshreeve@uidaho.edu

zhangjiaheng@hit.edu.cn

Notes

The authors declare no competing financial interest.

Acknowledgment

Financial support of the Office of Naval Research (N00014-16-1-2089), and the Defense Threat Reduction Agency (HDTRA 1-15-1-0028) is gratefully acknowledged. This work was supported by the National Natural Science Foundation of China (21905069), the Shenzhen Science and Technology Innovation Committee (JCYJ20180507183907224, KQTD20170809110344233), Economic, Trade and Information Commission of Shenzhen Municipality through the Graphene Manufacture Innovation Center (201901161514) and Guangdong Province Covid-19 Pandemic Control Research Fund 2020KZDZX1220.

References

[1] J. P. Agrawal, R. D. Hodgson, Organic Chemistry of Explosives, John Wiley & Sons Ltd, 2007.

[2] Q. Wu, W. Zhu, H. Xiao, A new design strategy for high-energy low-sensitivity explosives: combining oxygen balance equal to zero, a combination of nitro and amino groups, and N-oxide in one molecule of 1-amino-5-nitrotetrazole-3 N-oxide. J. Mater. Chem. A, 2 (2014): 13006-13015.

[3] X. X. Zhao, S. H. Li, Y. Wang, Y. C. Li, F. Q. Zhao, S. P. Pang, Design and synthesis of energetic materials towards high density and positive oxygen balance by N-dinitromethyl functionalization of nitroazoles, J. Mater. Chem. A, 4 (2016), 5495–5504.

[4] Q. Yu, P. Yin, J. Zhang, C. He, G. H. Imler, D. A. Parrish, J. M. Shreeve, Pushing the limits of oxygen balance in 1, 3, 4-oxadiazoles. J. Am. Chem. Soc, 139 (2017), 8816-8819.

[5] Y. Wang, Y. Liu, S. Song, Z. Yang, X. Qi, K. Wang, Y. Liu, Q. Zhang, Y. Tian, Accelerating the discovery of insensitive high-energy-density materials by a materials genome approach. Nat. Commun, 9 (2018): 1-11.

[6] J. Zhang, Q. Zhang, T. T. Vo, D. A. Parrish, J. M. Shreeve, M. Energetic salts with π-stacking and hydrogen-bonding interactions lead the way to future energetic materials. J. Am. Chem. Soc, 137(2015), 1697-1704.

[7] J. Zhang, J. Zhang, D. A. Parrish, J. M. Shreeve, Desensitization of the dinitromethyl group: molecular/crystalline factors that affect the sensitivities of energetic materials. J. Mater. Chem. A, 6 (2018), 22705-22712.

[8] V. Thottempudi, H. Gao, J. M. Shreeve, Trinitromethyl-substituted 5-nitro-or 3-azo-1, 2, 4-triazoles: synthesis, characterization, and energetic properties. J. Am. Chem. Soc,133 (2011), 6464-6471.

[9] G. Hervé, C. Roussel, H. Graindorge, Selective Preparation of 3, 4, 5-Trinitro-1H-Pyrazole: A Stable All-Carbon-Nitrated Arene. Angew. Chem. Int. Ed, 49 (2010), 3177-3181.

[10] P. Pagoria, M. X. Zhang, N. Zuckerman, G. Lee, A. Mitchell, A. DeHope, , A. Gash, C. Coon, P. Gallagher, Synthetic Studies of 2, 6-Diamino-3, 5-Dinitropyrazine-1-Oxide (LLM-105) from Discovery to Multi-Kilogram Scale. Propellants Explos. Pyrotech, 43 (2018), 15-27.

[11] O. Bolton, A. J. Matzger, Improved stability and smart-material functionality realized in an energetic cocrystal. Angew. Chem. Int. Ed, 50 (2011): 8960-8963.

[12] K. B. Landenberger, O. Bolton, A. J. Matzger, Energetic–energetic cocrystals of diacetone diperoxide (DADP): dramatic and divergent sensitivity modifications via cocrystallization. J. Am. Chem. Soc, 137 (2015): 5074-5079.

[13] O. Bolton, L. R. Simke, P. F. Pagoria, A. J. Matzger, High power explosive with good sensitivity: a 2: 1 cocrystal of CL-20: HMX. Cryst. Growth Des, 12 (2012), 4311-4314.

[14] Z. Yang, H. Wang, J. Zhang, Y. Ma, Y. Tan, F. Nie, J. Zhang, H. Li, Rapid Cocrystallization by Exploiting Differential Solubility: An Efficient and Scalable Process toward Easily Fabricating Energetic Cocrystals. Cryst. Growth Des, 20 (2020), 2129-2134.

[15] J. C. Bennion, N. Chowdhury, J. W. Kampf, A. J. Matzger, Hydrogen Peroxide Solvates of 2, 4, 6, 8, 10, 12-Hexanitro-2, 4, 6, 8, 10, 12-hexaazaisowurtzitane. Angew. Chem. Int. Ed, 55 (2016), 13118-13121.

[16] R. A. Wiscons, M. K. Bellas, J. C. Bennion, A. J. Matzger, Detonation Performance of Ten Forms of 5, 5′-Dinitro-2 H, 2 H′-3, 3′-bi-1, 2, 4-triazole (DNBT). Cryst. Growth Des, 18 (2018), 7701-7707.

[17] M. K. Bellas, A. J. Matzger, Achieving Balanced Energetics through Cocrystallization. Angew. Chem. Int. Ed, 58 (2019), 17185-17188.

[18] J. Xu, S. Zheng, S. Huang, Y. Tian, Y. Liu, H. Zhang, J. Sun, Host–guest energetic materials constructed by incorporating oxidizing gas molecules into an organic lattice cavity toward achieving highly-energetic and low-sensitivity performance. Chem. Commun, 55 (2019), 909-912.

[19] Y. Wang, S. Song, C. Huang, X. Qi, K. Wang, Y. Liu, Q. Zhang, Hunting for advanced high-energy-density materials with well-balanced energy and safety through an energetic host–guest inclusion strategy. J. Mater. Chem. A, 7 (2019), 19248-19257.

[20] S. Venkatachalam, G. Santhosh, K. Ninan, An overview on the synthetic routes and properties of ammonium dinitramide (ADN) and other dinitramide salts. Propellants Explos. Pyrotech, 29(3) (2004), 178-187.

[21] H. Gao, J. M. Shreeve, Azole-based energetic salts. Chem. Rev, 111 (2011), 7377-7436.

[22] J. Zhang, J. M. Shreeve, Time for pairing: cocrystals as advanced energetic materials. Cryst. Eng. Comm., 18 (2016), 6124-6133.

[23] M. A. Yousef, V. R. Vangala, Pharmaceutical Cocrystals: Molecules, Crystals, Formulations, Medicines. Cryst. Growth Des., 19 (2019), 7420-7438.

[24] J. F. Remenar, S. L. Morissette, M. L. Peterson, B. Moulton, J. M. MacPhee, H. R. Guzmán, Ö. Almarsson,. Crystal engineering of novel cocrystals of a triazole drug with 1, 4-dicarboxylic acids. J. Am. Chem. Soc, 125(2003), 8456-8457.

[25] H. G. Brittain, Cocrystal systems of pharmaceutical interest: 2011. Cryst. Growth Des., 12(2012), 5823-5832.

[26] V. S. Bryantsev, M. S. Diallo, A. C. van Duin, W. A. Goddard III, Evaluation of B3LYP, X3LYP, and M06-class density functionals for predicting the binding energies of neutral, protonated, and deprotonated water clusters. J. Chem. Theory. Comput, 5 (2009), 1016-1026.

[27] C. He, J. Zhang, J. M. Shreeve, Dense Iodine-Rich Compounds with Low Detonation Pressures as Biocidal Agents. Chem. Eur. J, 19 (2013), 7503-7509.

[28] G. Zhao, C. He, W. Zhou, J. P. Hooper, G. H. Imler, D. A. Parrish,J. M.Shreeve, Control of biohazards: a high performance energetic polycyclized iodine-containing biocide, Inorg. Chem. 57 (2018), 8673-8680.

[29] G. Zhao, C. He, D. Kumar, J. P. Hooper, G. H. Imler, D. A. Parrish, J. M. Shreeve, 1, 3, 5-Triiodo-2, 4, 6-trinitrobenzene (TITNB) from benzene: Balancing performance and high thermal stability of functional energetic materials, Chem. Eng. J., 378 (2019), 122119.

[30] C. He，J. P. Hooper, J. M. Shreeve, Iodine-rich imidazolium iodate and periodate salts: en route to single-based biocidal agents, Inorg. Chem. 55 (2016), 12844-12850.

[31] C. He, G. Zhao, J. P. Hooper, J. M. Shreeve, Energy and biocides storage compounds: synthesis and characterization of energetic bridged bis (triiodoazoles), Inorg. Chem. 56 (2017), 13547-13552.

[32] G. S. James, Lange's handbook of chemistry. CD & W Inc, Wyoming, 2005.

[33] J. P. Guthrie, Hydrolysis of esters of oxy acids: p K a values for strong acids; Brønsted relationship for attack of water at methyl; free energies of hydrolysis of esters of oxy acids; and a linear relationship between free energy of hydrolysis and p K a holding over a range of 20 p K units. Can. J. Chem, 56 (1978), 2342-2354.

[34] F. Lu, Y. Dong, T. Fei, J. Liu, H. Su, S. Li, S. Pang, Noncovalent Modification of 4, 4′-Azo-1, 2, 4-triazole Backbone via Cocrystallization with Polynitroazoles. Cryst. Growth Des, 19 (2019), 7206-7216.

[35] Y. Zhang, Y. Huang, D. A. Parrish, J. M. Shreeve, 4-Amino-3, 5-dinitropyrazolate salts—highly insensitive energetic materials. J. Mater. Chem, 21 (2011), 6891-6897.

[36] H. Xue, B. Twamley, J. M. Shreeve, Energetic quaternary salts containing bi (1, 2, 4-triazoles). Inorg. Chem, 44 (2005), 7009-7013.

[37] I. L. Dalinger, I. A. Vatsadze, T. K. Shkineva, G. P. Popova, S. A. Shevelev, Y. V. Nelyubina, Synthesis and Comparison of the Reactivity of 3, 4, 5-1H-Trinitropyrazole and Its N-Methyl Derivative. J. Heterocyclic. Chem, 50 (2013), 911-924.

[38] M. J. Frisch, et al. Gaussian 03, Revision E.01; Gaussian, Inc.: Wallingford, CT, 2004.

[39] J. D. Cox, D. D. Wagman, V. A. Medvedev, CODATA Key Values for Thermodynamics, Hemisphere Publishing Corp, New York, 1989.

[40] B. Delley, An all-electron numerical method for solving the local density functional for polyatomic molecules. J. Chem. Phys. 92 (1990), 508-517.

[41] B. Delley, From molecules to solids with the DMol 3 approach. J. Chem. Phys. 113 (2000), 7756-7764.

[42] P. Lu, Y. Wu, H. Kang, H. Wei, H. Liu, M. Fang, What can pKa and NBO charges of the ligands tell us about the water and thermal stability of metal organic frameworks? J. Mater. Chem. A, 2 (2014), 16250-16267.

[43] M. Z. Griffiths, I. Alkorta, P. L. Popelier, Predicting pKa values in aqueous solution for the guanidine functional group from gas phase ab initio bond lengths. Mol. Inform, 32 (2013), 363-376.

[44] M. Hakimi, M. Maeder, G. A. Lawrance, Synthesis, characterization, and crystal structure of a tricadmium complex of 3, 4-diamino-5-methyl-1, 2, 4-triazole. J. Coord. Chem, 64 (2011), 105-114.

[45] J. Zhang, D. A. Parrish, J. M. Shreeve, Curious cases of 3, 6-dinitropyrazolo [4, 3-c] pyrazole-based energetic cocrystals with high nitrogen content: an alternative to salt formation. Chem. Commun., 51 (2015), 7337-7340.

[46] J. Zhang, D. A. Parrish, J. M. Shreeve, Thermally Stable 3, 6-Dinitropyrazolo [4, 3-c] pyrazole-based Energetic Materials. Chem– Asian. J, 9 (2014), 2953-2960.

[47] C. Qi, S. H. Li, Y. C. Li, Y. Wang, X. K. Chen, S. P. Pang, A novel stable high-nitrogen energetic material: 4, 4′-azobis (1, 2, 4-triazole). J. Mater. Chem. A, 21 (2011), 3221-3225.

[48] F. Lu, E. Wang, J. Huang, M. Huang, F. Nie, F. X. Chen, The synthesis, property and reduction of high-nitrogen compound 3, 3′, 5, 5′-tetraazido-4, 4′-bis (1, 2, 4-triazole). Polyhedron, 117 (2016), 445-452.

[49] C. C.Unger, T. M.Klapötke, B. Z. Krumm, Unusual Energetic Periodate, Sulfate and Amino-bistetrazolate Salts of the Trinitropropylammonium Cation, Z. Anorg. Allg. Chem. 646(2020), 2-4.

[50] D. Chand, C. He, J. P. Hooper, L. A. Mitchell, D. A. Parrish, J. M. Shreeve, Mono-and diiodo-1, 2, 3-triazoles and their mono nitro derivatives. Dalton Trans, 45(2016), 9684-9688.

[51] G. Zhao, D. Kumar, C. He, J. P. Hooper, G. H. Imler, D. A.Parrish , J. M. Shreeve, New Generation Agent Defeat Weapons: Energetic N, N′-Ethylene-Bridged Polyiodoazoles. Chem. Eur. J, 23(2017), 16753-16757.

[52] M. J. Kamlet, S. J. Jacobs, The Chemistry of Detonations. 1. A Simple Method for Calculating Detonations Properties of CHNO Explosives. J. Chem. Phys. 48(1968), 23-35.

TOC Graphic

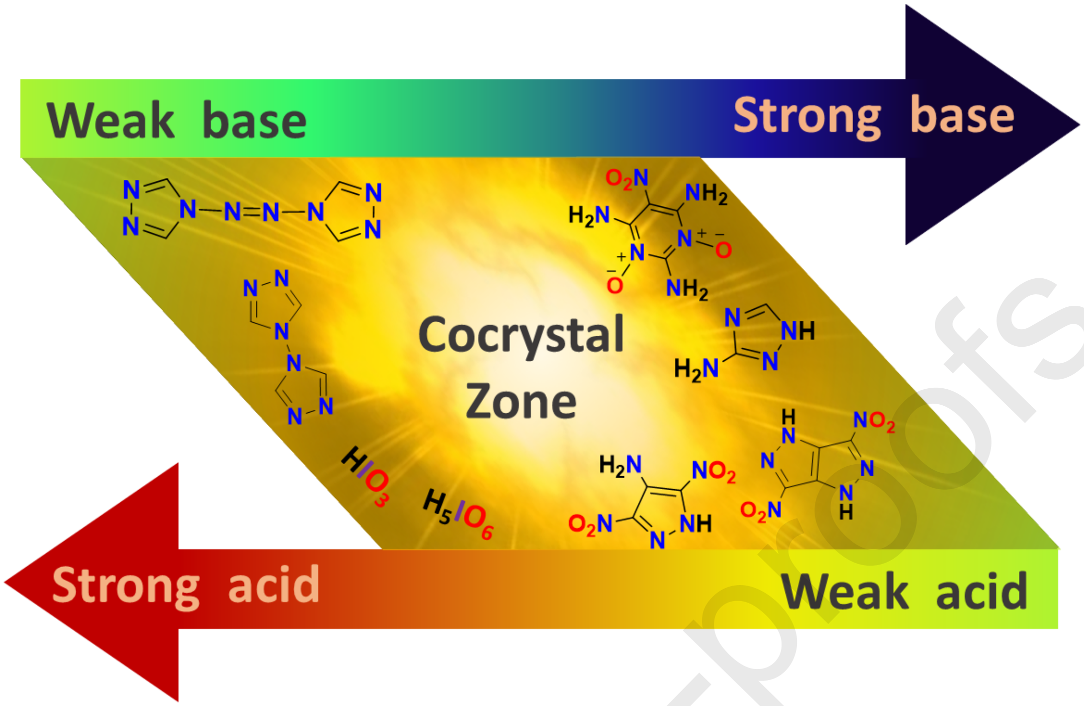
Weak base
Strong base
Cocrystal Zone
Strong acid
Weak acid
HIO3
H5IO6
O2N
NH2
H2N
NO2
NH

Highlights:

(1) Oxygen-rich acids, H_5IO_6/HIO_3, were introduced into energetics through cocrystallization of close acid-base gap.

(2) The available oxygen content carried by oxidant in cocrystal **3** is as high as 5.

(3) The excellent detonation properties of **3** and **4** makes them very promising as biocidal agents and high-energy materials.

(4) This study provides a new route for preparing cocrystals and broadens application of oxidants for the development of well-balanced energetic materials.